Journal of Applied Research in Science and Humanities

Wastewater treatment using polymeric nanocomposite membranes.

تنقية مياه الصرف الصحي باستخدام اغشية بوليمرية نانونية

Caroline Youssef, Marina Ebrahim , Neama Hafez, Norhan Mahdy, Norhan Mansour, Omnia Fahmy,

Ain Shams University, Faculty of Education, Bachelor's program in Science and Education (Primary)

Supervisor: Dr. Mervat Ismail Mohammed

Assistant Professor, Department of Physics, Faculty of Education, Ain Shams University

Abstract

In this study, Mn_2O_3 /PVC, Polyvinyl chloride polymer doped with various Mn_2O_3 nanoparticles, is prepared, and characterized. Solution casting was used to create Mn_2O_3/PVC polymeric nanocomposite films. The X-ray diffraction method verified that the Mn_2O_3NPs were effectively disseminated in PVC matrix with a single-phase structure. The casting process is expected to cause Mn_2O_3 nanoparticles in the PVC matrix to aggregate. According to UV/Vis/IR analysis, the optical energy gap values decrease as Mn_2O_3 NPs concentration increases. This indicates that complexes of charge transfer between the polymer and Mn^{+3}-ions are developing. Mn_2O_3/PVC nanocomposite can function as a photocatalyst to enhance the efficiency of Carmine dye photodegradation. The most effective Mn_2O_3/PVC nanocomposite film for the visible photocatalysis of Carmine dye is 2.5 wt% Mn_2O_3/PVC. Mn_2O_3/PVC has been shown to be a promising material for use in photocatalytic, and optoelectronic.

Key Words:

manganese oxide -doped PVC· Nanocomposite films · Optical analysis · Photodegradation process.

1. **Introduction**: Water pollution caused by harmful pollutants like industrial dyes and pesticides is a significant cause of environmental deterioration worldwide. Discharging industrial waste and synthetic dyes into the environment has led to widespread contamination in various regions. In textile manufacturing, a significant portion of dye production is lost as effluent, contributing to the pollution of water bodies (Menazea, 2020). These dyes can have detrimental effects on both the environment and human health. Many dyes are non–biodegradable, meaning they remain in ecosystems for long periods. Moreover, harmful byproducts can be produced when these dyes undergo certain reactions in wastewater(Fayek,2023).

The accumulation of these compounds poses a serious threat to the environment and public health. It is crucial to implement innovative technologies for removing dyes from industrial wastewater. By doing so, we can reduce freshwater contamination and safeguard the health of ecosystems and communities that rely on clean water sources (Houas,2001). The need for recycling and reusing wastewater is growing due to the world's finite freshwater supply. Less than 1% of the Earth's surface comprises easily accessible freshwater sources that are fit for human use, even though over 70% of the planet is covered in water (UN Water, 2022). Global freshwater use has been increasing at a rate that is more than twice as fast as population growth, and by 2050, it is predicted that overall water demand will have increased by 20–30% over current levels (WWAP, 2021). In many regions of the world, this increasing demand for freshwater and pervasive pollution from industrial, sewage, and agricultural sources is causing acute water stress (UNESCO, 2022). Efficient wastewater treatment and reuse techniques are crucial to increasing freshwater availability and decreasing harmful discharges (Takeuchi, 2020; Tsade Kara, 2021). United Nations, Water "UN World Water Development Report 2020." United States of America: New York, NY (2020).

Due to their growing interest, numerous studies have been conducted on nanocomposites embedded in polymer matrices (Rouabah, 2021). Owing to its interesting features and potential uses, single polymer matrix materials are among the most attractive material classes. Polymer nanocomposites are an advanced new technology with many applications and no negative environmental impacts. Furthermore, the composition, form, size, orientation, concentration, volume fraction, degree of dispersion of the nanoparticles, and interfacial bonding in the polymer matrix

all affect the effective properties of polymer nanocomposites (Roy S, 2016). In general, inorganic particles in polymer matrix enhance nanocomposites' mechanical, thermal, electrical, magnetic, and redox characteristics (Meti S, 2020). Transition metal oxides are a wide class of oxides with significant characteristics that are being studied in various categories (Julien C, 2017; Guo W, 2019; Shi X, 2018; Li X, 2017; Le Q, 2017; Zhao J, 2017; Shalini A, 2019). As an n–type non–stoichiometric semiconductor, manganese oxide (MnO, MnO_2, Mn_2O_3, Mn_3O_4, and Mn_5O_8) can exist in a variety of polymorphic and crystallographic forms and oxidation states, with 1D, 2D, and 3D morphologies such as rods, wires, cubes, spheres, urchins, sheets, flowers, and many more. Some preparation techniques, such as the sol–gel method, electrospinning, solid state, ion exchange, precipitation and co–precipitation techniques, and thermal decomposition, could synthesize manganese oxide based on previous reports (Zhang L, 2018; Zhang S, 2016; Kumar N, 2017; Wang Y, 2016; Zhang Y, 2018; Qi S, 2008; Paulraj P, 2021).

Polymers are the most extensively utilized materials because of their low cost and simplicity of processing. They are, therefore, regarded as adaptable, advantageous, and cost–effective due to their wide range of functions (Rouabah, 2021; Gulati U, 2012). PVC and other polymers have garnered much interest in many facets of life. PVC has attracted interest due to its favorable characteristics, superior mechanical qualities, and rigidity compared to other common thermoplastic polymers. PVC has the benefit of being easily bio undegradable and non–toxic in the environment. PVC has also been found to have useful uses in the antimicrobial and industrial sectors (Yıldırım OA, 2013; Hosseini SM, 2015).

The process of photocatalysis in Mn_2O_3/PVC nanocomposite films involves the absorption of light by manganese oxide (Mn_2O_3) nanoparticles embedded within the film. When these nanoparticles are exposed to light, they create electron–hole pairs, which then interact with molecules in the environment through redox reactions. Previous research utilizing various scavengers has identified $^{\bullet}O_2^-$ and $^{\bullet}OH$ radicals as the primary species responsible for breaking down Carmine dye. The generated electrons and holes are transferred to the surface of the photocatalyst. The electrons reduce oxygen (O_2) to form superoxide radical anions ($^{\bullet}O_2^-$), while the holes either oxidize water (H_2O) to form hydroxyl radicals ($^{\bullet}OH$) or directly oxidize Carmine dye. These reactive species ($^{\bullet}O_2^-$, $^{\bullet}OH$, and h^+) initiate the redox reactions that break down Carmine dye into carbon dioxide (CO_2), and water (H_2O). Consequently, the solution of Carmine dye loses its color as the aromatic rings degrade. Furthermore,

research has indicated that the significance of different species in the photocatalysis process decreases in the following order: electrons (e^-) > superoxide radical anions ($^{\bullet}O_2^-$) > hydroxyl radicals ($^{\bullet}OH$) > holes (h^+) (Jagodi´c, 2023).

The effect of Mn_2O_3 nanofillers on the PVC matrix is investigated in this article. X-ray diffraction (XRD) was investigated. The influence of the amount of Mn_2O_3 nanoparticles, optical bandgap analysis, transmittance, and absorption in the investigated nanocomposite films was tightly regulated. Mn_2O_3/PVC has much greater photocatalytic activity than pure PVC. This could be because Mn_2O_3 and PVC work so well together. A visible photocatalytic mechanism for Mn_2O_3/PVC nanocomposite films was also suggested and researched.

2. The Theoretical Framework

The literature on the photocatalytic performance of PVC and the polymeric Mn_2O_3/PVC nanocomposite highlights the potential of these materials for environmental remediation and other applications. Studies have shown that PVC itself has limited photocatalytic activity, but when combined with Mn_2O_3 nanoparticles in a nanocomposite structure, the photocatalytic performance can be significantly enhanced. The presence of Mn_2O_3 nanoparticles in the PVC matrix allows for the generation of reactive oxygen species under light irradiation, leading to improved degradation of organic pollutants.

Changjun (Yang,2011)"Enhanced Solid–Phase Photocatalytic Degradation Activity of a Poly(vinyl chloride)–TiO_2 Nanocomposite". Film with Bismuth Oxyiodide Film of PVC–BiOI/TiO_2 photodegradable nanocomposite film was synthesized. UV–Vis spectroscopy was used to study the solid–phase photocatalytic degradation behavior under UV light irradiation. Concerning photocatalytic degradation activity, the PVC–BiOI/TiO_2 nanocomposite film showed more activity. It was discovered that 0.75% was the ideal mass ratio for BiOI to TiO_2. After 336 hours of radiation, the weight loss rate of the PVC–BiOI/TiO_2 nanocomposite film was 30.8%, 1.5 times higher than that of the PVC–TiO_2 nanocomposite film under the same conditions.

(Rouabah. N,2020)"Structural, Optical and Photocatalytic Properties of PVC/CdS Nanocomposites Prepared by Soft Chemistry Method" The study explores the use of (CdS) embedded in a polymeric polyvinylchloride (PVC) matrix for the degradation of MB under UV light irradiation. A direct energy bandgap between 4.07 eV and 3.85 eV is revealed by the UV–vis spectroscopy, which also shows that the transmission is between 80 and 95% in the visible region. The photocatalytic study demonstrated the potential of PVC/CdS nanocomposites for MB degradation under UV light irradiation.

(Rouabah .N, 2021) "Nanocomposite synthesis of silver doped magnesium oxide

incorporated in PVC matrix for photocatalytic applications" This study describes the spin coating procedure used to prepare the Ag:MgO/PVC nanocomposite. PVC and pure MgO/PVC have direct band gap energies. As the concentration of Ag:MgO increases, the band gap energy value decreases. Under UV light irradiation, the photocatalytic activity of this nanocomposite film was assessed for the methylene blue (MB) dye. The outcome showed that Ag:MgO/PVC nanocomposite films have good potential for MB degradation.

(Nouhad Rouabah ,2023) "Synthesis of a thin film of CuO/MgO/PVC nanocomposites for Photocatalytic applications". This study examines the impact of 5% and 15% CuO/MgO mixed in a (PVC) matrix on photocatalytic activity. In 15% CuO/MgO/PVC NCs, the bandgap energy of MgO/PVC decreased dramatically from 4.00 eV to 3.77 eV. This work also shows the great capacity of CuO/MgO/PVC thin films towards the photodegradation of methylene blue (MB) dye. MB dye photodegradation was compared, and the results showed that the photocatalysis was superior by 15%, with an efficiency of approximately 44% at a rate constant of 5.20×10^{-3} min^{-1}.

(Jagodić, I ,2023) "The photodegradation of methylene blue (MB) under simulated sunlight was studied". In this work various iron(III) oxide/titanium(IV) oxide/polyvinyl chloride (Fe2O3/TiO2/PVC) nanocomposites in tablet form. The maximum photocatalytic efficiency was attained when 70.6% of the MB was eliminated in the presence of Fe_2O_3/TiO_2/PVC. Furthermore, the indicated photocatalyst's potential for photo-cleaning and reuse was also investigated. It is evident from the data that after five iterations, the activity did not decline.

3.Methods of Research and the tools used.

3.1. Preparation of Mn_2O_3 nanoparticles

The sol-gel process was used to create Mn_2O_3. After thoroughly mixing, a specific amount of Mn $(NO_3)_3$ was mixed with the appropriate citric acid amount in a volume of distilled water of 30 ml. **The** solution was then held at 110 °C until the weight was constant. Finally, the temperature was raised to 550 °C for two hours (see Scheme 1a).

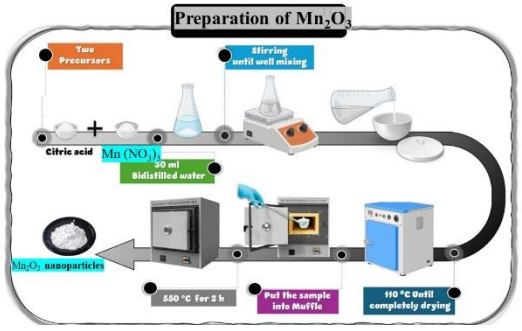

Scheme.1a: Preparation of Mn_2O_3 nanoparticles.

3.2. Preparation of Mn_2O_3/PVC polymeric nanocomposites films

To create films made of Mn_2O_3/PVC polymeric nanocomposite, the solution casting procedure was used. 20 g of PVC powder is dissolved in 200 ml of high-grade Tetrahydrofuran THF using magnetic stirring at a speed of 700 rpm for 48 hours at room temperature. By means of an ultrasonic homogenizer used for 5 minutes at 100 W,

different weight percents of Mn_2O_3 (0, 0.05, 0.25, 0.5, and 2.5 wt %) were equally disseminated in the PVC solution. The casting of pure and Mn_2O_3/PVC solutions was done in a flat-bottomed Petri dish, which was then kept in a dark place until it dried completely. After five days, all Mn_2O_3/PVC films were removed from the Petri dish (see Scheme 1b).

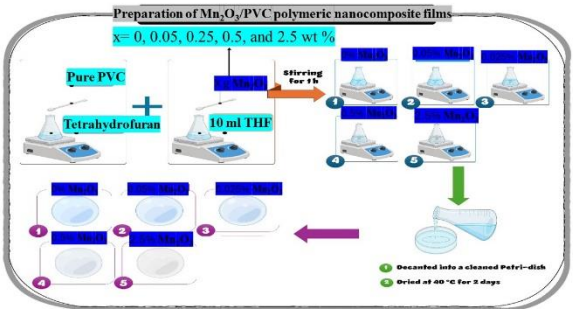

Scheme.1b: PVC/ Mn_2O_3nanocomposites preparation

3.3. Measurement techniques

The XRD patterns of Mn_2O_3/PVC films were collected by employing a Shimadzu LabX-XRD-6000 with CuK_α (CuK_α = 1.5406A°). By using the JASCO V-570 spectrometer at room temperature and 200 to 2500 nm in wavelength, linear optical characteristics were achieved.

3.4. Photocatalytic activity studies

Using a wood photoreactor, the photocatalytic validity of each produced sample has been evaluated. I.S. Yahia and his group created the photoreactor at NLEBA, Ain Shams University (ASU) (Hussien, 2020). Mn_2O_3/PVC membranes were mixed with 200 ml of an aqueous mixture containing 0.01g/L of carmine dye and 1 mL of H_2O_2 at room temperature. The generated solution was combined with Mn_2O_3/PVC and held for 30 minutes in complete darkness to attain the adsorption-desorption equilibrium. UV_A light was used to irradiate the fluid during the experiment. After irradiation, 3 ml of the suspension was removed from the mixture every 10 minutes. The measurement of the change in dye absorbance during photodegradation was done using the absorbance at a maximum wavelength of 665 nm. A UV-Vis spectrophotometer was used to measure absorbance data/plots to evaluate carmine dye's degradation rate (see Fig. 1&Table 1).

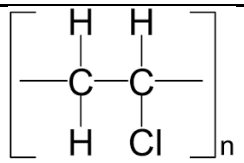	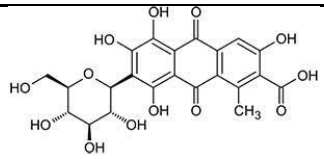
(a) PVC polymer	(b) **carmine dye**

Table 1: The structure of (a) PVC polymer, and (b) carmine dye

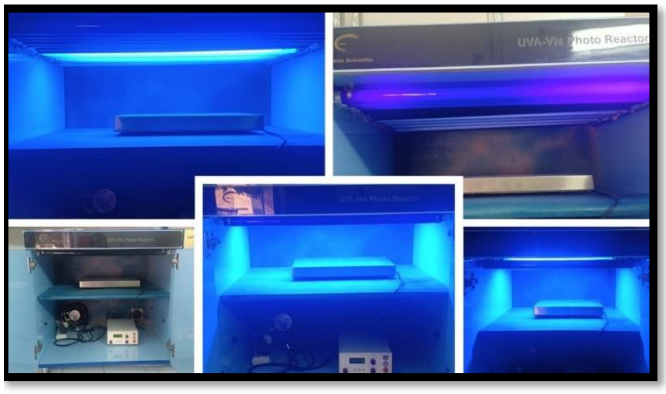

Fig. 1: Photoreactor design and operation in NLEBA, Ain Shams University, Cairo, Egypt.

4. Results of Research

4.1. Mn_2O_3/PVC nanocomposites films structural analysis.

The XRD spectra for pure PVC and Mn_2O_3 /PVC nanocomposite films have been evaluated, as shown in Fig. 2, for investigating the influence of Mn_2O_3 NPs content on the amorphous PVC polymer chain. The diffraction pattern observed for pure PVC exhibits two broad humps at 2θ values of 15° and 25° with their intensity decreasing systematically, which confirms the amorphous nature of the PVC polymer (Guedri, 2020; Abouhaswa AS, 2020). The XRD patterns of Mn_2O_3 /PVC nanocomposite films studied here show that there are no peaks corresponding to crystalline peaks of Mn_2O_3, which infers that the Mn_2O_3 NPs are completely dissociated in their solutions prepared for the preparation of films. The formation of strong complexes between C-Cl of PVC and the cation Mn^{+3} of Mn_2O_3 results in complete dissociation of the Mn_2O_3, which agrees with earlier studies (Khorsand Zaka A, 2010). In the polymeric host, adding NPs changes the intensity and width of the initial humps. The rise in width or intensity reduction shows that the crystallinity of the PVC polymer changes (decrease). It could indicate that certain interactions can take place between the polymer chains and the NPs (Augustin M, 2015).

Table 2: The indirect and direct band gap, and the band tails energy of Urbach's for pure PVC film and its Mn_2O_3 nanofiller doped PVC polymeric nanocomposite films.

Samples	E_g (eV) Indirect		E_g (eV) Direct		E_u, (meV)
Pure PVC	3.91	2.98	4.08	---	8.81
0.05 wt% Mn_2O_3	3.74	2.82	4.03	2.33	11.98
0.25 wt% Mn_2O_3	3.57	2.76	3.85	3.23	22.49
0. 5 wt% Mn_2O_3	3.35	2.66	4.72	3.17	86.58
2.5 wt% Mn_2O_3	3.1	1.95	3.51	2.88	102.14

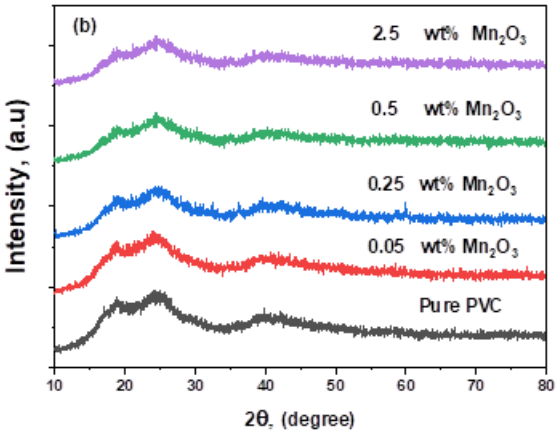

Fig. 2: XRD spectra for PVC/Mn_2O_3 nanocomposites.

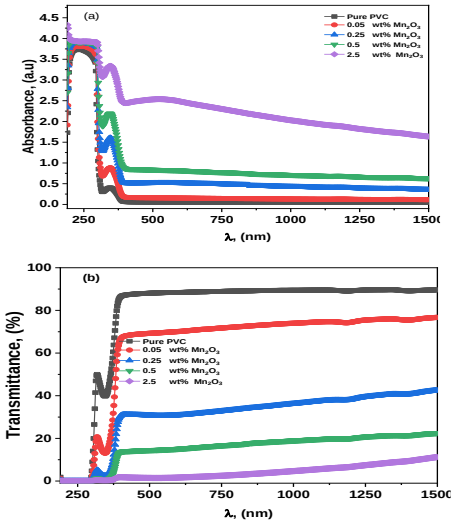

Fig.3. optical UV-Vis-NIR (a) Transmittance curves and (b) Absorbance of Mn_2O_3 /PVC nanocomposite films.

4.2. UV-Vis-IR analysis of Mn_2O_3 /PVC nanocomposite membranes.

The UV/vis absorption spectra of the produced pure PVC and the Mn_2O_3/PVC nanocomposites at wavelengths between 190 and 1500 nm are shown in Fig.3a. Pure PVC film's measured spectra show two absorption bands at 235 and 347 nm. The π–π* electronic transition, often known as the 234–362 nm absorption band, is responsible (Mudassir Hasana, 2015). The increase in absorbance could be detected using the C-Cl bond (Al-Muntaser A.A, 2020) . PVC has the least amount of absorption in the UV, Vis, and NIR spectrums. Additionally, the absorption of manganese oxide-free electrons to the radiation causes the absorption peak's intensity to increase with a greater Mn_2O_3 %.

Additionally, the peak positions have somewhat changed after adding Mn_2O_3 to PVC, demonstrating the interaction between the PVC matrix and Mn_2O_3 nanoparticles as demonstrated by XRD at various concentrations**.**

Fig. 3b displays the transmission of PVC/ Mn_2O_3 nanocomposites in the UV-Vis-IR light spectrum. Approximately 88% of pure PVC transmits data; however, transmittance decreases when Mn_2O_3 NP concentration increases. The transmittance spectrum decreases as the ratio of Mn_2O_3 nanoparticles increases inside the matrix (Ismail A.M, 2020). The spectrum intensity of PVC is

continuously reduced with nanoparticle levels from 88 % to roughly 5% due to complex interaction between the nanoparticles and matrix via the C-Cl connection The absorption coefficient ($\boldsymbol{\alpha}$), Urbach energy ($\boldsymbol{E_U}$), band gap (E_g), and the kind of the material's electronic transitions have all been identified from the spectra of polymer films' optical absorption. The following equation may be used to determine the polymer films' absorption coefficient (Hussien, 2020);

$$\boldsymbol{\alpha} = \frac{\boldsymbol{2.3Abs}}{\boldsymbol{d}} \qquad (1)$$

where d is the film thickness, and Abs is the film absorbance. Tauc's equation (**Tauc J, 1974)** may be used to figure out the optical band gap.

$$\boldsymbol{\alpha h\upsilon = B(h\upsilon - E_g)^m} \qquad (2)$$

where hυ is the energy of the incident photon, B is constant, and E_g is the optical band gap dependent on the value of the variable parameter m for both potential transitions, direct and indirect (m = 1/2 and 2 for allowed direct and allowed indirect transitions, respectively). The direct (E_{gd}) and indirect (E_{gind}) optical band gap are figured out at the *hυ*-axis from the point at which the straight component of the curves extrapolates to zero absorption [$(\alpha h\upsilon)^{2}$ or $(\alpha h\upsilon)^{1/2} = 0$] as displayed in Fig. 4a (direct state) and Fig. 4b (indirect state). Table 2 gives an overview of the determined values. As the Mn_2O_3 concentration in the PVC matrix rises, it is shown that the direct and indirect band gaps fall from 5.8 to 4.8 eV and from 4.8 to 4.05 eV, respectively. The increase in localized states that resulted from Mn_2O_3 injection into the PVC matrix can be credited to this. For every sample examined, it is discovered that the E_{gd} values are higher than the E_{gind} values. Two zones corresponding to the absorption edges show the linear portion dependency for pure PVC. The transitions between the HOMO and LUMO bands were responsible for the multi-band gaps that were characterized in terms of optical absorption spectra. Table 2 demonstrates that the optical band gap's values drop with increasing Mn_2O_3 content.

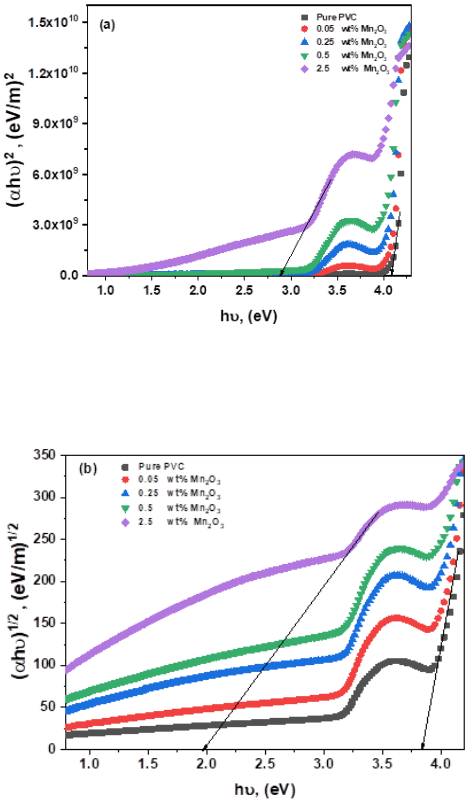

Fig. 4: Plots of (a) ($\alpha\ h\nu$)^2 versus photons energy *hν*, and (b) ($\alpha\ h\nu$)$^{1/2}$ versus *hν* for Mn_2O_3 /PVC nanocomposite films.

The relationship between the absorption coefficient and photon energy at the lower photon energy of the optical band gap is seen in the following equation (tail absorption). (Hussien, 2020);:

$$\alpha = \alpha_o \exp\left(\frac{h\nu}{E_U}\right) \qquad (3)$$

where ، α_o is a constant

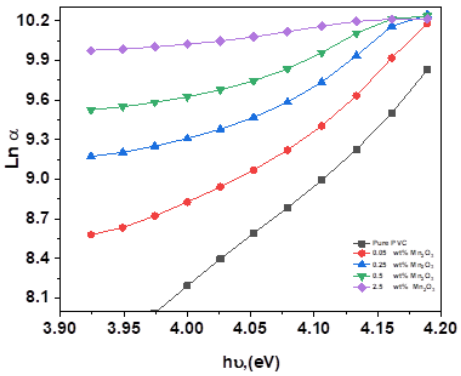

Fig. 5: Plots of ln α versus $h\nu$ for the Mn_2O_3 /PVC nanocomposite films.

The relationship between the rise in E_U and the concentration of Mn_2O_3 is described in Table 2 using the estimated slope values from Fig. 5, which supports the rise in the amorphous nature of the films. The E_U increase may be caused by creating Mn_2O_3/PVC nanocomposite polymeric films with a highly structured Mn_2O_3 aggregation. Because the particles get bigger, the rise in E_U values is related to the growth in Mn_2O_3 clusters. The findings of this spectroscopic investigation demonstrated that the decrease in crystalline size may be linked with the XRD patterns and a lowering in the energy gap.

4.3. Efficiency and kinetics of photocatalysis

The degradation of Carmine dye in an aqueous solution under UVA light irradiation was used to evaluate the photocatalytic efficiency of Mn_2O_3/PVC polymeric composites. The photocatalytic performance of PVC and the polymeric Mn_2O_3/PVC composite was also evaluated for comparison. The UV-visible absorption spectra of Carmine dye over the recently prepared photocatalyst are shown to exposure time in (Fig. 6). In the absorption spectrum, the pure Carmine dye's absorption peak can be seen at 520 nm (π to π^*). The colour of the dye solution shifted from dark red powder to colorless when exposed to sunlight; however, the dye solution in complete darkness displayed essentially no colour change (Hussien M.S.A, 2020).. It is clear from (Fig. 6) that all samples' intensities decrease over time, indicating that the effectiveness of dye photodegradation increased over time.

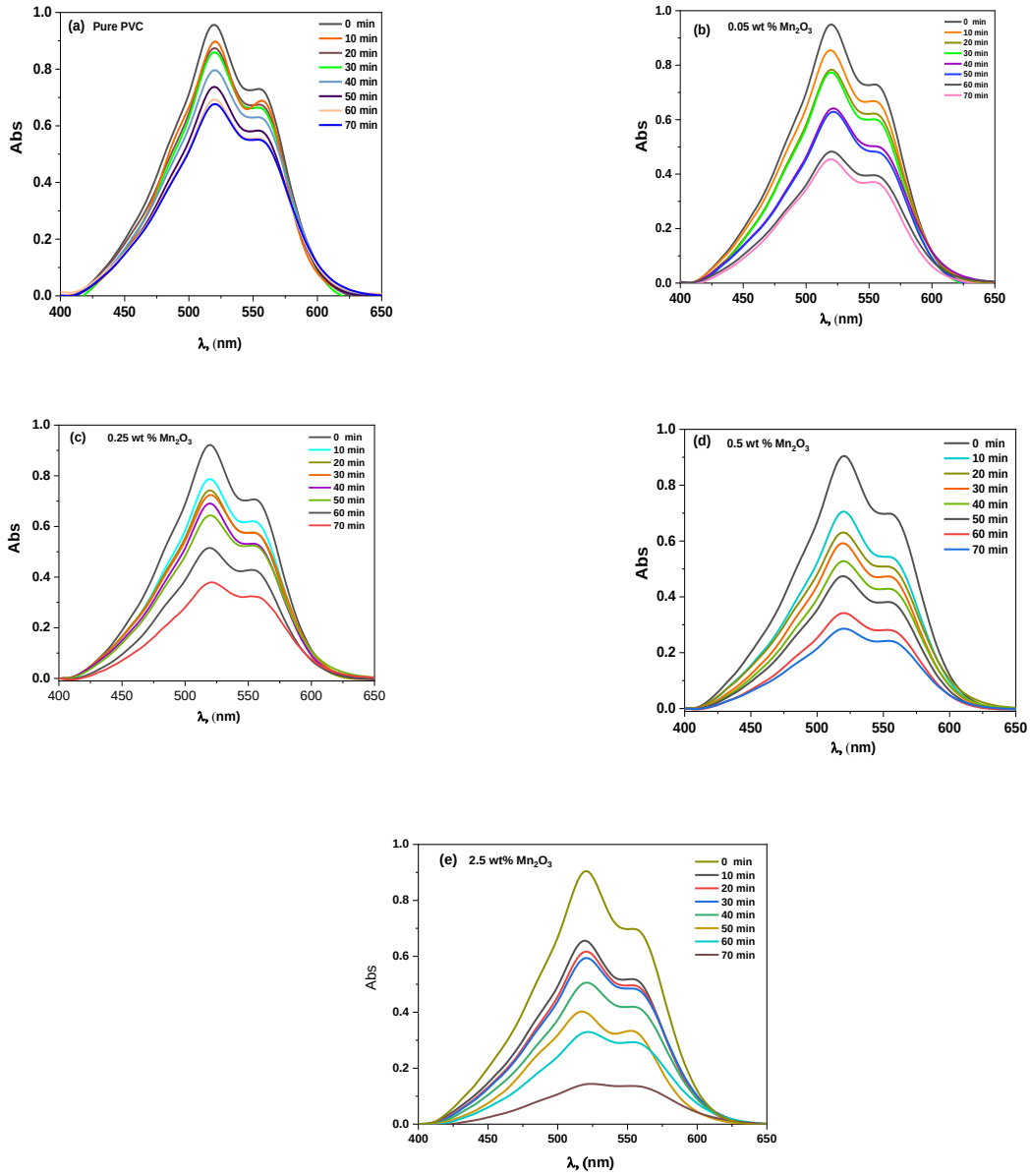

Fig. 6: Absorption spectra of Carmine dye with Mn_2O_3/PVC polymeric nanocomposites.

The absorbance data were then used to calculate the degradation rate, as shown in Fig. 6. The pseudo-first-order kinetics for Carmine dye degradation was calculated as follows (Hussien M.S.A, 2020):

$$ln(A/A_o) = -kt, \quad (4)$$

Where the constant rate is k (min^{-1}), Where: A_o & A (mg L^{-1}) are absorption at 0 min illumination and at irradiation time, respectively , and at time t (min). The reaction rate has reached the maximum while using 2.5 wt% Mn_2O_3/ PVC photocatalyst, indicating Mn_2O_3 is an effective photocatalyst. This performance is significantly increased after increasing Mn_2O_3 concentration in the PVC sheet. According to (Fig. 7a), the Mn_2O_3 content had the following effects on the photodegradation rate: Pure PVC (0.00496 min^{-1}), 0.05wt% Mn_2O_3 (0.00903 min^{-1}), 0.25wt% Mn_2O_3 (0.01106 min^{-1}), 0. 5wt% Mn_2O_3 (0.01538 min^{-1}), and 2.5wt% Mn_2O_3 (0.02003 min^{-1}), respectively.

The collective of morphological and optical effects is primarily responsible for the increased rate constant of the reaction using Mn_2O_3/PVC sheets. Adding Mn_2O_3 NPs into PVC polymer changed their electronic structure, resulting in a decrease in the bandgap value. The presence of Mn_2O_3 also increases the rate of adsorbed O_2 molecules and OH ions on the surface of the membrane. The majority of the photoexcited electrons and holes have been formed and reacted to form activated radicals. The obtained radicals are powerful oxidizers that can break up Carmine's chemical bonds and produce the colorless solution, leading to degraded molecules (Hussien, 2020). Fig. 7b depicts the change in % degradation as a function of irradiation time. The following relationship was used to determine % degradation (Hammani S, 2018):

$$\% \text{ of degradation} = (Ao-A/Ao) \times 100\%, \quad (5)$$

It depicts the photocatalytic degradation of Carmine dye on Mn_2O_3/PVC with various Mn_2O_3 contents using an in-situ UV-lamp as a function of irradiation times. The percentage of Carmine dye degraded by Mn_2O_3 /PVC varies depending on the Mn_2O_3 content. It also showed how the Mn_2O_3 concentration affects the photodegradation reaction after 70 min of exposure. The addition of Mn_2O_3 to the photocatalytic process of Carmine dye degradation can significantly improve photocatalytic efficiency. The degradation rate increases with increasing Mn_2O_3 content, with 2.5 wt% Mn_2O_3/PVC achieving the optimum degradation. When a photon with an energy equal to or higher than the energy band gap of Mn_2O_3 is absorbed, electron hold pairs (e_{cb}-/h_{vb}+) are formed. Superoxide ($\bullet O_2^-$) and hydroxyl radicals ($^{\bullet}OH$). are created during the photochemical reaction of holes and electrons with oxygen. Reactive radicals do the same thing: they are responsible for the photodegradation process (Yang, 2011; Rouabah, N, 2021). Due to the photogenerated recombination taking place between the e^- -h^+ conduction band of Mn_2O_3 and the valence band of Mn_2O_3 being reduced

(Rouabah, N, 2021), Mn_2O_3/PVC nanocomposites were applied for Carmine dye degradation. At a 522 nm of Carmine dye solution was used to determine the time-dependent variation of Carmine dye concentration, we found that it became proportional to the absorbance.

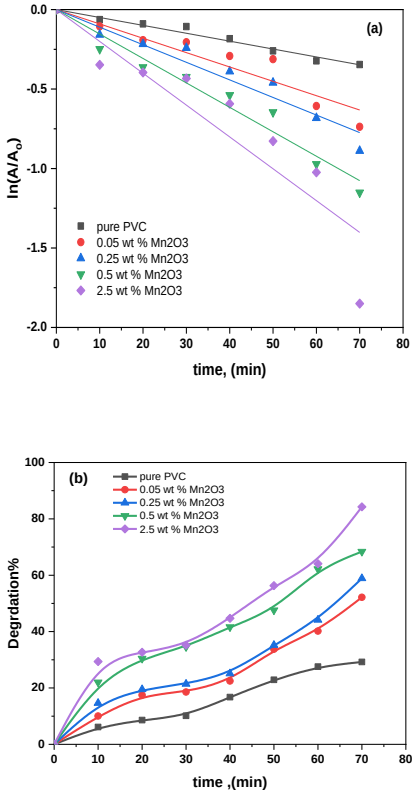

Fig.7: (a) kinetic study of carmine dye photodegradation, and(b) % Degradation of carmine dye.

The photocatalytic activity of Mn_2O_3/PVC sheets is shown in Fig. 8. It was shown that the Carmine dye concentration degradation was attributed to Mn_2O_3/ PVC photocatalytic activity. Mn_2O_3 predominantly influences it; without Mn_2O_3, Adsorption didn't take place. Even though Mn_2O_3 nanoparticles have been agglomerated and embedded in the polymer, with a part of their surface is exposed to water, the samples show significant activity. The entire dye degradation was demonstrated within 70 minutes of UVA light irradiation, showcasing the excellent catalytic activity of 2.5wt% Mn_2O_3. The optical studies are consistent with the photocatalytic output. Due to the superior heterostructure formed between the Mn_2O_3 nanoparticles and the PVC matrix(Mohammed, M.I., 2024), the reaction rate is increased for 2.5wt% Mn_2O_3 more than it was for the 0.05wt% Mn_2O_3 sample.

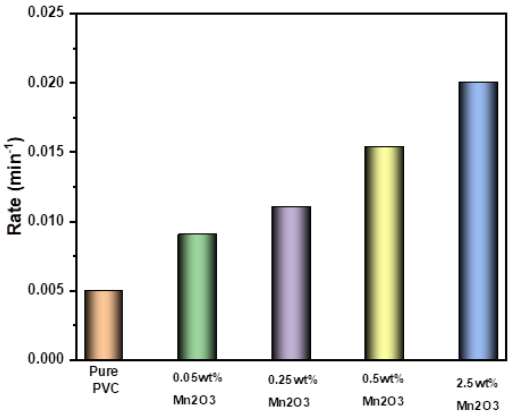

Fig.8: kinetic rate of Carmine dye with Mn_2O_3/PVC polymeric nanocomposites.

Trapping agents and Proposed photodegradation mechanism of Carmine dye using Mn_2O_3/PVC nanocomposites.

As the photons of visible light, Carmine dye with the catalyst photoelectrons and photo holes produced (e^- and h^+). Also, $^{-}O_2\cdot$ can be produced due to the reaction between photoelectron and O_2 in air. Also,$\cdot O_2H$ can be formed through the reaction between $^{-}O_2\cdot$ and H^+.$\cdot OH$ obtained from ^{-}OH of water or catalyst surface with h^+ (Rouabah,

N., 2021). From the previous work, it was confirmed that the photodegradation mechanism occurs through radicals and holes (h^+ and $^{-}O_2^{\cdot}$). As demonstrated above, the possible mechanisms of Carmine dye (Mohammed, M.I., 2024) photodegradation using Mn_2O_3/PVC in the presence of UVA light irradiation were as follows:

$$Mn_2O_3/PVC + h\upsilon \rightarrow Mn_2O_3/PVC\ (h^+ + e^-) \quad (6)$$

$$\text{Carmine dye} + h\upsilon \rightarrow \text{Carmine dye}^{*+} + e^- \quad (7)$$

$$O_2 + e^- \rightarrow {}^{-}O_2^{\cdot} \quad (8)$$

$${}^{-}O_2^{\cdot} + 2H^+ + 2\,e^- \rightarrow H_2O_2 \quad (9)$$

$$H_2O_2 + e^- \rightarrow {}^{\cdot}OH + {}^{-}OH \quad (10)$$

$$({}^{\cdot}OH / {}^{-}O_2^{\cdot}) + \text{Carmine dye} \rightarrow products \quad (11)$$

$$(h^+ / H_2O_2) + \text{Carmine dye} \rightarrow CO_2 + H_2O \quad (12)$$

5. Conclusion

A simple combustion and casting approach successfully produces Mn_2O_3 nanoparticles and nanocomposites made of PVC. Through XRD, the strong interface interactions and collaborations between the various levels of Mn_2O_3 and the PVC matrix are verified. When additional Mn_2O_3 nanoparticles are added to the matrix, the absorbance measurements show a high absorption of UV-Vis light. Shifting the absorption edges to lower photon energies predicts how nanoparticles would affect a host polymer's bandgap. With increasing Mn_2O_3 concentration, it was discovered that the direct and indirect optical band gaps dropped. The Mn_2O_3 nanoparticle addition may have caused localized states to form in the band gap, explaining the decrease in E_g behaviour. Because of the disorder of PVC caused by Mn_2O_3 doping, Urbach energy E_u behaves inversely to E_g. Evaluation and consideration are given to the use of PVC/ Mn_2O_3 nanocomposites and their photocatalysis efficiency. These films are also superb photocatalysts for regulating environmentally friendly photodegradable polymer materials. In conclusion, the findings show that the nanometric Mn_2O_3 may significantly enhance PVC and improve its optical, structural, and photocatalytic capabilities.

Acknowledgement

We would like to thank Dr. **Mervat Ismail Mohammed** for proposing her scientific ideas about this work and for her guidance, support, understanding and patience while working on this project. Also we would like to thank **Professor Dr. Heba Al-Gharib Attia**, Head of the Physics Department, Professor **Dr. Hanan Helmy**, Head of the Biology Department, and **I.S. Yahia and his group at NLEBA**, **Ain Shams University** (**ASU**) for their support, advice and assistance during our work on the graduation project.

References and Sources

Abouhaswa AS and Taha TA 2020 Tailoring the optical and dielectric properties of PVC/CuO nanocomposites Polym. Bull. 77 6005–16

Al–Muntaser A.A, Abdelghany A.M, Abdelrazek E.M, Elshahawy A.G, (2020) Enhancement of optical and electrical properties of PVC/PMMA blend films

doped with $Li_4Ti_5O_{12}$ nanoparticles, Journal of Materials Research and Technology,9, 1,,789–797, https://doi.org/10.1016/j.jmrt.2019.11.019.

Augustin M, Fenske D, Bardenhagen I, Westphal A, Knipper M, Plaggenborg T, Kolny-Olesiak J, Parisi J, Beilstein J. Nanotechnol. (2015) 6, 47–59

Fayek, N., Khalafallah, A. (2023) Advancing Environmental Monitoring : Unveiling Heavy Metal Contamination with Calibration-Free Picosecond Laser-Induced Breakdown Spectroscopy (CF-PS-LIBS). 0–20

Guedri A, Zaabat M, Boudine B and Hafdallah A (2020) Synthesis, characterization, structural, and optical properties of polyvinyl chloride/zinc oxide nanocomposite films for photocatalysis application J. Inorg. Organomet. Polym. Mater. 30 4884–94

Gulati U, Rajesh UC, Rawat DS, Zaleski JM (2012) Development of magnesium oxide–silver hybrid nanocatalysts for synergistic carbon dioxide activation to afford esters and Heterocycles at Ambient Pressure. J. N ame.00:1–3. https://doi.org/10.1039/C9GC04040D

Guo W, Yu C, Li S, Wang Z, Yu J, Huang H, Qiu J, (2019) Strategies and insights towards the intrinsic capacitive properties of MnO_2 for supercapacitors: Challenges and perspectives, Nano Energy. 57 459–472.

Hammani S, Barhoum A, Bechelany M.F, (2018). Fabrication of PMMA/ZnO nanocomposite: effect of high nanoparticles loading on the optical and thermal properties. J. Mater. Sci. Compos. https://doi.org/10.1007/s10853-017-1654-9

Hosseini SM, Abdolhosseini I. Kameli SP, Salamati H (2015) Effect of Ag doping on structural, optical and photocatalytic properties of ZnO nanoparticles. J Alloys Compd 640:408–415 https://doi.org/10.1016/j.jallcom.2015.03.136.

Houas, A., Lachheb, H., Ksibi, M., Elaloui, E., Guillard, C., Herrmann, J.M. (2001). Photocatalytic degradation pathway of methylene blue in water. Appl. Catal. B Environ. 31, 145–157 . https://doi.org/10.1016/S0926-3373(00)00276-9

Hussien, M.S.A., Mohammed, M.I. & Yahia, I.S. (2020) Flexible photocatalytic membrane based on CdS/PMMA polymeric nanocomposite films: multifunctional materials. *Environ Sci Pollut Res* 27, 45225–45237

https://doi.org/10.1007/s11356-020-10305-1

Hussien Mai S.A, Mohammed M.I, Yahia I.S.(2020) Multifunctional Applications of Graphene-Doped PMMA Nanocomposite Membranes for Environmental Photocatalytic. Journal of Inorganic and Organometallic Polymers and Materials .https://doi.org/10.1007/s10904-019-01433-4

Ismail A.M, Mohamed El-Newehy H, Mehrez El-Naggar E, Meera Moydeen A, Menazea A.A, 2020 Enhancement the electrical conductivity of the synthesized polyvinylidene fluoride/polyvinyl chloride composite doped with palladium nanoparticles via laser ablation, Journal of Materials Research and Technology,9, 5,11178-11188, https://doi.org/10.1016/j.jmrt.2020.08.013.

Jagodi´c, I.; Guth, I.; Luki´c-Petrovi´c, S.; Tamindžija, D.; Šoji´c Merkulov, D.; Fin˘cur, N.; Bognár, S.; Putnik, P.; Bani´c, N. (2023) Reusable Fe_2O_3/TiO_2/PVC Photocatalysts for the Removal of Methylene Blue in the Presence of Simulated Solar Radiation. *Nanomaterials*, *13*, 460. https://doi.org/10.3390/ nano13030460.

Jagodić, Ivana, Imre Guth, Svetlana Lukić-Petrović, Dragana Tamindžija, Daniela Šojić Merkulov, Nina Finčur, Szabolcs Bognár, Predrag Putnik, and Nemanja Banić. 2023. "Reusable Fe_2O_3/TiO_2/PVC Photocatalysts for the Removal of Methylene Blue in the Presence of Simulated Solar Radiation" *Nanomaterials* 13, no. 3: 460. https://doi.org/10.3390/nano13030460

Julien C, Mauger A, (2017) Nanostructured MnO2 as Electrode Materials for Energy Storage, Nanomaterials. 7 396.

Khorsand Zaka A, Abd Majid W .H, Abrishami M .E, Yousefi R, 2010 X-ray analysis of ZnO nanoparticles by Williamson–Hall and sizestrain plot methods. Solid State Sci. 13, 251–256. https :// doi.org/10.1016/j.solid state scien ces..11.024

Kumar N, Bhaumik S, Sen A, Shukla A. P, Pathak S. D, (2017) One-pot synthesis and firstprinciples elasticity analysis of polymorphic MnO2 nanorods for tribological assessment as friction modifiers. RSC Adv. 7 34138-34148.

Le Q . J, Wang T, Tran D. N. H, Dong F, Zhang Y .X, Losic D, (2017) Morphology-controlled MnO2 modified silicon diatoms for high-performance asymmetric supercapacitors, J. Mater. Chem. A, 5 10856-10865.

Li X, Ding R, Shi W, Xu Q, Wang L, Jiang H, Yang Z, Liu E, (2017) Hierarchical mesoporous Ni–P@MnO_2 composite for high performance supercapacitors. Mater. Lett. 187 144–147.

Menazea, A.A., Ezzat, H.A., Omara, W., Basyouni, O.H., Ibrahim, S.A., Mohamed, A.A., Tawfik, W., Ibrahim, M.A. , (2020). Chitosan/graphene oxide composite as an effective removal of Ni, Cu, As, Cd and Pb from wastewater. Comput. Theor. Chem. 1189 https://doi.org/10.1016/j.comptc.2020.112980

Meti S, Bhat UK, Rahman MR (2020) Colossal dielectric permittivity of Nylon–6 matrix–based composites with nano–TiO_2 fillers. Applied Physics A 126:264. https://doi.org/10.1007/s00339–020–3445–4

Mohammed, M.I., Yahia I.S., Elfiky, D. *et al.* (2024). Structural, Bandgap Analysis, Electrical Properties, and Photocatalytic Applications of PMMA/Nd_2O_3 Composite Membranes: Towards Multifunctional Materials for Optoelectronic and Environmental Applications. *J Inorg Organomet Polym* 34, 848–863. https://doi.org/10.1007/s10904–023–02839–x

Mudassir Hasana , Rajeev Kumar, Barakatbn M .A, Moonyong Lee. (2015) Synthesis of PVC/CNT nanocomposite Fibers using simple deposition technique for the application of Alizarin Red S (ARS) removal , RSC Advances · DOI: 10.1039/x0xx00000x

Paulraj P, Ahmad U, Rajendran K, Manikandan A, Sathamraja A, Kumar R, Manikandan E, Pandian K, Baskoutas S, Hassan A, Ahmed A. Ibrahim, Mabkhoot A. Alsaiari, (2021) Methylene blue intercalated layered MnO_2 nanosheets for high–sensitive nonenzymatic ascorbic acid sensor, J. Mater Sci: Mater Electron, 3 1–13

Qi S. Y, Feng J, Yan J, Hou X. Y, Zhang M. L, (2008) Hydrothermal synthesis and supercapacitor properties of urchin sphere and nanowire MnO_2. Chin. J. Nonferrous Met. 18 113–117.

Rouabah, N., Boudine, B., Nazir, R. *et al,* (2021), Nanocomposite synthesis of silver doped magnesium oxide incorporated in PVC matrix for photocatalytic applications. *J Polym Res* 28, 154.https://doi.org/10.1007/s10965–021–02516–y.

Rouabah, N., Boudine, B., Nazir, R. *et al.* (2021). Nanocomposite synthesis of silver doped magnesium oxide incorporated in PVC matrix for photocatalytic applications. *J Polym Res* 28, 154 https://doi.org/10.1007/s10965–021–02516–y

Rouabah, N., Boudine, B., Nazir, R. *et al.* (2021). Nanocomposite synthesis of silver doped magnesium oxide incorporated in PVC matrix for photocatalytic applications. *J Polym Res* 28, 154 https://doi.org/10.1007/s10965-021-02516-y

Rouabah, N., Boudine, B., Nazir, R. *et al.* (2021). Structural, Optical and Photocatalytic Properties of PVC/CdS Nanocomposites Prepared by Soft Chemistry Method. *J Inorg Organomet Polym* 31, 1102–1110 https://doi.org/10.1007/s10904-020-01752-x

Rouabah, Nouhad, Nazir, Roshan, Djaballah, Yassine, Mir, AbQayoom, Ameur, Imene, & Beldjebli, Ouidad. (2023). Synthesis of a thin film of CuO/MgO/PVC nanocomposites for Photocatalytic applications. IRANIAN JOURNAL OF CATALYSIS, 13(1), 23-34. SID. https://sid.ir/paper/1065074/en

Roy S, Srivastava SK, Mittal V (2016) Facile noncovalent assembly of MWCNT-LDH and CNF-LDHas reinforcing hybrid fillers in thermoplastic polyurethane/nitrile butadiene rubber blends. J Polym Res 23:36. https://doi.org/10.1007/s10965-016-0926-4.

Shalini A, Paulraj P, Pandian K, Anbazhagan G, Jaisankar V, (2019) Synthesis and Characterization of Graphene Oxide Coated Au Nano Particles and The Study of its Application on Electro Catalytic Activity of Nitric Oxide, Advanced Materials Proceedings, 4(4) 158-161.

Shi X, Li Y, Chen R, Ni H, Zhan W, Zhang B, Zheng F, Dong S, (2018) Defective carbon nanotube forest grown on stainless steel encapsulated in MnO_2 nanosheets for supercapacitors. Electrochim. Acta 278 61-71.

Takeuchi, H., Tanaka, H. (2020). Water reuse and recycling in Japan — History, current situation, and future perspectives. Water Cycle. 1, 1–12 https://doi.org/10.1016/j.watcyc.2020.05.001

Tauc J, 1974 Amorphous and Liquid Semiconductors, Plenum Press, London, New York, p. 171.

Tsade Kara, H., Anshebo, S.T., Sabir, F.K., Adam Workineh, G. (2021). Removal of Methylene Blue Dye from Wastewater Using Periodiated Modified Nanocellulose. Int. J. Chem. Eng. 2021, https://doi.org/10.1155/2021/9965452 .

Wang Y, Ding P, Wang C, (2016) Fabrication and lithium storage properties

of MnO2 hierarchical hollow cubes. J. Alloys Compd. 654 273–279.

Yang, C., Deng, K., Peng, T., & Zan, L. (2011). Enhanced Solid–Phase Photocatalytic Degradation Activity of a Poly(vinyl chloride)–TiO_2 Nanocomposite Film with Bismuth Oxyiodide. *Chemical Engineering & Technology*, *34*(6), 886–892. https://doi.org/10.1002/ceat.201000450

Yıldırım OA, Unalan HE, Durucan C (2013) Highly Efficient Room Temperature Synthesis of Silver–Doped Zinc Oxide(ZnO:Ag) Nanoparticles: Structural, Optical, and Photocatalytic Properties. J Am Ceram Soc 96(3) 766–773. https://doi.org/10.1111/jace.12218

Zhang L, Chen Q, Han X, Zhang Q. (2018) MnO_2 Nanoparticles and Carbon Nanofibers Nanocomposites with High Sensing Performance Toward Glucose. Journal of Cluster Science 29 1089–1098.

Zhang S, Zheng J, (2016) Synthesis of single–crystal a–MnO_2 nanotubes–loaded Ag@C core– shell matrix and their application for electrochemical sensing of nonenzymatic hydrogen peroxide. Talanta 159 231–237.